American Journal of Pathology, Vol. 163, No. 6, December 2003

Peritubular Capillary Loss after Mouse Acute Nephrotoxicity Correlates with Down-Regulation of Vascular Endothelial Growth Factor-A and Hypoxia-Inducible Factor-1α

Hai-Tao Yuan, Xiao-Zhong Li, Jolanta E. Pitera, David A. Long, and Adrian S. Woolf

From the Nephro-Urology Unit, Institute of Child Health, University College London, London, United Kingdom

Although the response of kidneys acutely damaged by ischemia or toxins is dominated by epithelial destruction and regeneration, other studies have begun to define abnormalities in the cell biology of the renal microcirculation, especially with regard to peritubular capillaries. We explored the integrity of peritubular capillaries in relation to expression of vascular endothelial growth factor (VEGF)-A, hypoxia-inducible factor (HIF)-α proteins, and von Hippel-Lindau protein (pVHL) in mouse folic acid nephropathy, a model in which acute tubular damage is followed by partial regeneration and progression to patchy chronic histological damage. Throughout a period of 14 days, in areas of cortical tubular atrophy and interstitial fibrosis, loss of VEGFR-2 and platelet endothelial cell adhesion molecule-expressing peritubular capillaries was preceded by marked decreases in VEGF-A transcript and protein levels. Nephrotoxicity was associated with tissue hypoxia, especially in regenerating tubules, as assessed by an established *in situ* method. Despite the hypoxia, levels of HIF-1α, a protein known to up-regulate VEGF-A, were reduced. During the course of nephrotoxicity, levels of pVHL, a factor that destabilizes HIF-1α, increased significantly. We speculate that that down-regulation of VEGF-A may be functionally-implicated in the progressive attrition of peritubular capillaries in areas of tubular atrophy and interstitial fibrosis; VEGF-A down-regulation correlates with a loss of HIF-1α expression which itself occurs in the face of increased tissue hypoxia. ***(Am J Pathol 2003, 163:2289–2301)***

The response of kidneys acutely damaged by ischemia or toxins is dominated by epithelial destruction and regeneration.[1,2] Other studies, however, have begun to define abnormalities in the cell biology of the renal microcirculation, especially with regard to peritubular capillaries.[3–5] Indeed, it is increasingly appreciated that these vessels are also implicated in the pathobiology of chronic renal diseases,[6] including those triggered by acute injury or renal ablation.[7–12] Using animal models, a complex picture is emerging, in which peritubular capillaries can remodel after renal insults; this response consists of variable endothelial injury with proliferation/regeneration, sometimes followed by capillary loss. The response can be dominated by capillary growth[8] but when the balance favors progressive endothelial deletion there is an association with interstitial fibrosis.[7,10–12] Somewhat similar, but more limited, histological observations have been reported in human chronic kidney diseases, with some authors emphasizing overall capillary loss in a range of chronic nephropathies,[13,14] whereas others noting that peritubular capillaries are apparently increased, especially before severe fibrosis is established.[15]

Secreted growth factors drive the construction of, and maintain the integrity of, endothelia and capillary networks.[16] Vascular endothelial growth factor-A (VEGF-A) is one of the best studied of these molecules, signaling by binding to VEGF receptor-2 (VEGFR-2); there are, in addition, other molecules with similar roles, including VEGF-A-related proteins and the angiopoietins.[16] VEGF-A is expressed in normal adult human and murine kidneys, immunolocalizing to glomeruli and tubules,[8,10,17] and it is also detected at sites of angiogenesis and *in situ* vessel formation in embryonic kidneys.[18,19] The amount of VEGF-A protein expressed by a cell is controlled by several mechanisms, including regulation of transcription rate and transcript stability.[20] VEGF-A expression is up-regulated by hypoxia, an effect mediated through hypoxia-inducible factors (HIF), transcription factors that bind as heterodimers (eg, HIF-1α/HIF-β and HIF-2α/HIF-β) to a hypoxia-responsive element in DNA where they complex with other proteins to drive transcription.[21–23] The transcription of other genes

Supported by the Kidney Research Aid Fund (to H. T. Y. and D. A. L.), the National Kidney Research Fund (project grant R4/2/2001), the Medical Research Council (Ph.D. studentship to D. A. L.), and by the Chinese National Science Fund (grant 30271234 to X. Z. L.).

Accepted for publication August 15, 2003.

Address reprint requests to Dr. Hai-Tao Yuan, Nephro-Urology Unit, Institute of Child Health, University College London, 30 Guilford St., London WC1N 1EH, United Kingdom. E-mail: hyuan@ich.ucl.ac.uk.

expressed in the kidney, including heme oxygenase-1 (HO-1) and erythropoietin (EPO) are also up-regulated by HIF binding. HIF transcriptional activity is favored by hypoxic stabilization of HIF-α proteins because, in normoxia, they are hydroxylated and targeted for proteasomal degradation after binding to the von Hippel-Lindau protein (pVHL); renal carcinoma cell lines lacking pVHL express HIF-α maximally in normoxia.

The aim of the current experiments was to explore the relationship between the integrity of renal peritubular capillaries with VEGF-A expression, using a mouse model in which acute tubular necrosis is followed by partial regeneration and also progression to patchy cortical tubular atrophy and interstitial fibrosis. We used the folic acid (FA) model: intraperitoneal FA administration is followed by the rapid appearance of FA crystals in tubules and subsequent acute nephrotoxicity followed by patchy fibrosis.[5,24–26] Acute damage has been attributed to sudden blockade of individual tubules; however, alkalinization of urine by co-administration of $NaHCO_3$ decreases crystal deposition, but proximal tubular lesions still occurs, consistent with direct nephrotoxicity.[25] Our hypothesis was that capillary attenuation would occur in fibrotic areas and that this would be accompanied by down-regulation of VEGF-A proteins. Our experiments confirmed that loss of peritubular capillaries, visualized by immunostaining for VEGFR-2 and platelet endothelial cell adhesion molecule (PECAM), was preceded by profound falls of kidney VEGF-A mRNA and protein levels. We also discovered that the effects of FA nephrotoxicity on HIF-α proteins was complex, with decreased HIF-1α and increased HIF-2α, and that both changes occurred in the presence of increased tissue hypoxia, as assessed by an established *in situ* method;[12,27] furthermore, nephrotoxicity was followed by up-regulation of pVHL protein levels.

Materials and Methods

Reagents

Reagents were obtained from Sigma Chemical Co. (Poole, Dorset, UK) unless otherwise specified. Antibodies used were: goat anti-EPO (Sc-1310; Santa Cruz Biotechnology Inc., Santa Cruz, CA) raised against an epitope in human EPO amino-terminus, cross-reactive with mouse EPO; rabbit anti-HO-1 (Sc-10789, Santa Cruz Biotechnology Inc.) raised against amino acids 184 to 288 in human HO-1 carboxy (C)-terminus, cross-reactive with mouse HO-1; rabbit anti-HIF-1α (Sc-10790, Santa Cruz Biotechnology Inc.) raised against an epitope corresponding to amino acids 575 to 780 near the human HIF-1α C-terminus, cross-reactive with mouse HIF-1α; rabbit anti-HIF-2α (NB-100-122; Novus Biologicals Inc., Littleton, CO) raised against an epitope present in mouse and human HIF-2α, specific for HIF-2α *versus* HIF-1α; rabbit anti-VEGF-A (Sc-507, Santa Cruz Biotechnology Inc.) raised against amino acids 1 to 140 of human VEGF-A, cross-reactive with mouse VEGF-A; rabbit anti-pVHL (Sc-5575, Santa Cruz Biotechnology Inc.) raised against the 1 to 181 amino acid peptide representing full-length human pVHL, cross-reactive with mouse pVHL; rat anti-mouse PECAM (550274; Pharmingen, San Diego, CA) and VEGFR-2 (555307, Pharmingen); mouse anti-human α-smooth muscle actin (α-SMA) conjugated with horseradish peroxidase coupled to an inert polymer backbone (U7033; DAKO, High Wycombe, UK), cross-reactive with mouse α-SMA. The Hypoxyprobe-1 kit (Chemicon International Inc., Temecula, CA) utilizes pimonidazole hydrochloride, an established hypoxia marker;[27] areas of tissue hypoxia are detected *in situ* using an antibody (Hypoxyprobe-1MAb1) against pimonidazole adducts.

Experimental Model

Animal protocols were approved by the United Kingdom Home Office. Eight-week-old male CD1 mice (Charles Rivers Mouse Farms, UK) were administered FA (240 mg/kg) in vehicle (0.2 ml of 0.3 mol/L $NaHCO_3$) or vehicle-only by intraperitoneal injection. This FA dose reliably induces severe nephrotoxicity, as assessed by histology finding of grossly flattened renal epithelia after 24 hours, but had a morbidity of $<2\%$ throughout the experimental period.[5,26] Eight kidneys were analyzed before FA or vehicle-only administration (the control group). Other kidneys were harvested at 0.5, 1, 3, 7, and 14 days, with eight FA (the experimental groups) and eight vehicle (the sham groups) animals at each time point. In some experiments ($n = 4$ for each time point) Hypoxyprobe-1 was intraperitoneally injected at 60 mg/kg body weight in phosphate-buffered saline (PBS; pH 7.4) 1 hour before sacrifice. Mice were sacrificed by decapitation and kidneys removed within 1 minute. Left kidneys were used for routine histology, immunohistochemistry, and *in situ* hybridization; right kidneys were used for Northern, slot, and Western blots; in the latter case, organs were snap-frozen in liquid nitrogen.

Immunohistochemistry

Kidneys were fixed in 4% paraformaldehyde at 4°C overnight and embedded in paraffin and 5-μm or 7-μm sections were used for immunohistochemistry. Sections were dewaxed with Histoclear (Raymond Lamb, East Sussex, UK). Some deparaffinized sections were stained with Masson's trichrome in which collagen is stained blue, cytoplasm red, and nuclei black. Others were stained with periodic acid-Schiff to identify proximal tubule brush borders. Others sections were processed for immunohistochemistry as described[28] after treatment with either proteinase K, proteinase, or heat-retrieving buffer (pH 9.5; Pharmingen) for antigen retrieval. Endogenous peroxidase was quenched with 3% H_2O_2 for 30 minutes and sections were blocked in 10% bovine calf serum/0.1% Tween-20 in PBS. Sections were reacted overnight with antibodies (HIF-1α, 1:200; HIF-2α, 1:2000; PECAM, 1:1000; α-SMA, 1:4; VEGF, 1:400; VEGFR-2, 1:2000). Primary antibodies raised in rabbit were detected using the anti-rabbit Envision kit (DAKO), while those raised in

rat were detected using the anti-rabbit Envision kit after incubation with rabbit-anti rat IgG (Vector Laboratories, Burlingame, CA). Protein adducts of Hypoxyprobe-1 in hypoxic tissues were detected by Hypoxyprobe-1MAb1 and horseradish peroxidase-conjugated F(ab′)2 fragment of anti-mouse IgG antibody. Brown color was generated using diaminobenzidine as substrate. Negative controls comprised omission primary antibodies. Nuclei were counterstained with hematoxylin.

Quantitative Image Analysis of Cortical Capillaries and Fibrosis Using PECAM and Masson's Trichrome Staining

To quantify fibrosis we used the blue color generated by Masson's trichrome staining, and to quantify capillaries we used the brown color generated by PECAM immunostaining. Positive signal was captured using the Magic Wand Tool of Adobe Photoshop 5.5. For each group (control and experimental days 3 and 14), we analyzed data from six kidneys; for fibrosis, 10 random, low-power microscope fields were studied for each organ, and for capillaries 10 random, high-power filed were studied (for experimental day 14, regenerated and fibrotic areas were assessed individually). Signal area, expressed as a percentage of the whole image, was calculated using ImageJ software (*http://rsbweb.nih.gov/ij/*). The average value from the 10 random images for each organ was calculated.

In Situ *Hybridization*

Partial murine VEGF-A sequence (389 bp) was amplified and cloned into pGEM-T cDNA plasmid and confirmed by sequencing as described.[18] Plasmid was linearized with restriction enzymes and sense and anti-sense uridine triphosphate-digoxigenin-labeled riboprobes prepared using linearized plasmid cDNA as template, the appropriate RNA polymerase, and the conditions recommended in the Dig RNA labeling kit (Boehringer Mannheim, Sussex, UK). *In situ* hybridization was performed as described[29] with minor modifications. Paraffin-embedded sections (7 μm) were dewaxed with Histoclear, treated with proteinase K (20 μg/ml) at 37°C for 10 minutes, and postfixed in 4% paraformaldehyde. Sections were covered with 50 μl of prehybridization mix [50% v/v formamide, 5× standard saline citrate (SSC), 1× Denhardt's reagent, heat-denaturated salmon sperm DNA 0.1 mg/ml, 10% w/v dextran sulfate] for 30 minutes at 65°C, followed by 50 μl of the same mixture containing the digoxigenin-labeled riboprobe. A glass coverslip was applied and hybridization was allowed to occur at 65°C overnight. Sections were washed at 65°C with 25% formamide in 2× SSC for 1 hour, 1× SSC and 0.1% sodium dodecyl sulfate for 30 minutes, and 0.1× SSC and 0.1% sodium dodecyl sulfate for 30 minutes. Hybridized probe was detected by incubation with anti-digoxigenin antibody (1:1000) conjugated to alkaline phosphatase, followed by the chromogen solution, nitro blue tetrazolium, and 5-bromo-4-chloro-3-indolylphosphate toluidinum. Slides were washed and mounted with Citifluor (Chemical Labs., London, UK). Negative controls run in parallel with each experiment included sections without riboprobe added or hybridized in identical manner with a digoxigenin-labeled sense riboprobe; none of these controls showed staining above background under the conditions used for these experiments.

Slot and Northern Blots

Total RNA was isolated with Tri-Reagent and 20 μg of total RNA was denatured and transferred onto Hybond-N membrane (Amersham Pharmacia Biotech, Little Chalfont, Buckinghamshire, UK) using slot apparatus (Bio-Rad, Hemel Hempstead, Hertfordshire, UK) and fixed with UV-Stratalinker (Stratagene, La Jolla, CA). VEGF inserts were isolated after digesting with appropriate restriction enzymes and random primer labeling was performed with the Prime-a-Gene labeling system (Promega, Southampton, UK). Unincorporated labeled dCTP was removed by using a push-column (Stratagene, La Jolla, CA, USA). Blots were prehybridized with Quick-Hyb solution (Stratagene) at 65°C for 30 minutes and hybridized with specific probes at 65°C for 2 hours. After hybridization the filters were washed twice with 2× SSC at 65°C for 30 minutes and once with 0.1× SSC/0.1% sodium dodecyl sulfate at 65°C for 30 minutes. X-ray films were exposed to blots for 24 to 72 hours at −80°C. The blot was reprobed for 18S rRNA to use as a measure of loading of total RNA.[30] Using the same VEGF-A and 18S RNA probes, we also performed Northern blots, exactly as described,[31] resulting in a band at 3.9 kb.

Western Blotting

Kidneys were homogenized in radioimmunoprecipitation assay buffer (30 μl/ml of 2.2 mg/ml aprotinin, 10 μl/ml of 10 g/ml phenylmethyl sulfonyl fluoride, 10 μl/ml of 100 mmol/L sodium orthovanadate) at 4°C. Supernatants were collected after 30 minutes of centrifugation at 13,000 rpm and protein concentration was measured (BCA protein assay; Pierce, Rockford, IL). Protein (50 to 100 μg) was denaturated at 100°C for 5 minutes and separated on 8% or 15% sodium dodecyl sulfate-polyacrylamide electrophoresis gels. Ponceau S staining was used to visualize the equality of protein loading before proteins were transferred to nitrocellulose membranes (Amersham Pharmacia Biotech, Chalfont, Bucks, UK) by electroblotting (Bio-Rad, Hertfordshire, UK). Blots were blocked for 1 hour with 5% (w/v) fat-free milk powder, 0.1% bovine serum albumin, and 0.1% Tween-20 in PBS, and subsequently incubated with EPO, HIF-1α and HIF-2α, HO-1, VEGF-A, and pVHL antibodies at 4°C overnight. Blots were washed twice in PBS with 0.1% Tween-20 and once in blocking solution. They were then incubated for 30 minutes with anti-rabbit antibody conjugated with horseradish peroxidase or anti-goat conjugated with horseradish peroxidase, according to the primary antibody used. Immunoreactive bands were

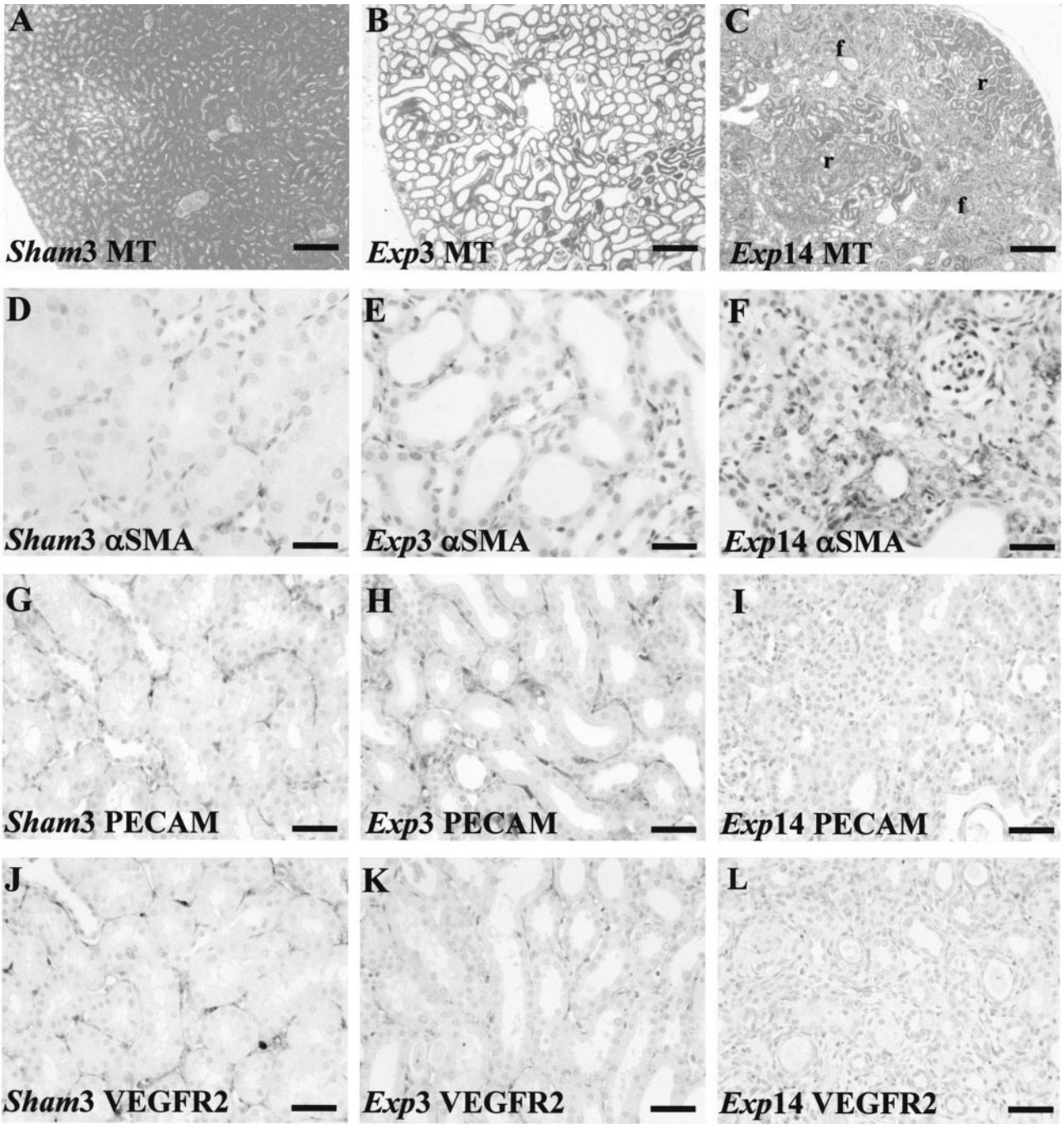

Figure 1. Effects of FA on gross morphology and endothelial markers. Typical views are shown from eight kidneys in each group. **A** to **C** and **M** to **O** were stained with Masson's trichrome; **D** to **L** were stained with hematoxylin; **D** to **F** were immunostained for α-SMA; **G** to **I** and **P** to **S** were immunostained for PECAM; **J** to **L** were immunostained for VEGFR2. **A:** Sham group day 3 (sham3). **B:** Widespread flattening of cortical tubule epithelia in the experimental group on day 3 (Exp3). **C:** On day 14, the cortex of experimental group (Exp14) showed regenerated (r) and fibrotic (f) areas. **D:** In a typical high-power field, barely any peritubular cells immunostained for α-SMA in sham kidneys. **E:** On experimental day 3, several cells between tubules express α-SMA. **F:** On experimental day 14, α-SMA immunostaining was marked in fibrotic areas. **G:** Cortical peritubular capillaries immunostained for PECAM in sham kidneys. **H:** On experimental day 3, PECAM immunoreactive vessels were noted between acutely damaged cortical tubules. **I:** On experimental day 14, PECAM immunostaining was attenuated in fibrotic areas. **J:** Cortical peritubular capillaries immunostained for VEGFR2 in sham kidneys. **K:** On experimental day 3, VEGFR2 immunoreactive vessels were also noted between acutely damaged cortical tubules. **L:** On experimental day 14, VEGFR2 immunostaining was attenuated in fibrotic areas. **M** to **O: Dotted lines** indicate outer border of cortex. These frames show the blue/fibrotic color generated by Masson's trichrome processed into black; note the extensive, patchy, fibrosis on experimental day 14 (**O**) *versus* the control (**M**) and experimental day 3 groups. **P** to **S:** These frames show the brown/capillary color from PECAM immunohistochemistry processed into black; note preservation of capillaries on experimental day 3 (**Q**) *versus* control (**P**); on experimental day 14, regenerated cortical zones show a modest reduction in signal (**R**), whereas virtually no signal was detected in fibrotic areas (**S**). **T:** Note increased cortical fibrosis area at experimental day 14. **U:** Note the modest fall in capillary area at experimental day 14 in regenerated locations (Exp14-R), and the major decrease of capillary area in fibrotic locations (Exp14-F). In **T** and **U** an **asterisk** indicates $P < 0.05$ *versus* control. Scale bars: 320 μm (**A–C**, **M–O**); 80 μm (**D–L**, **P–S**).

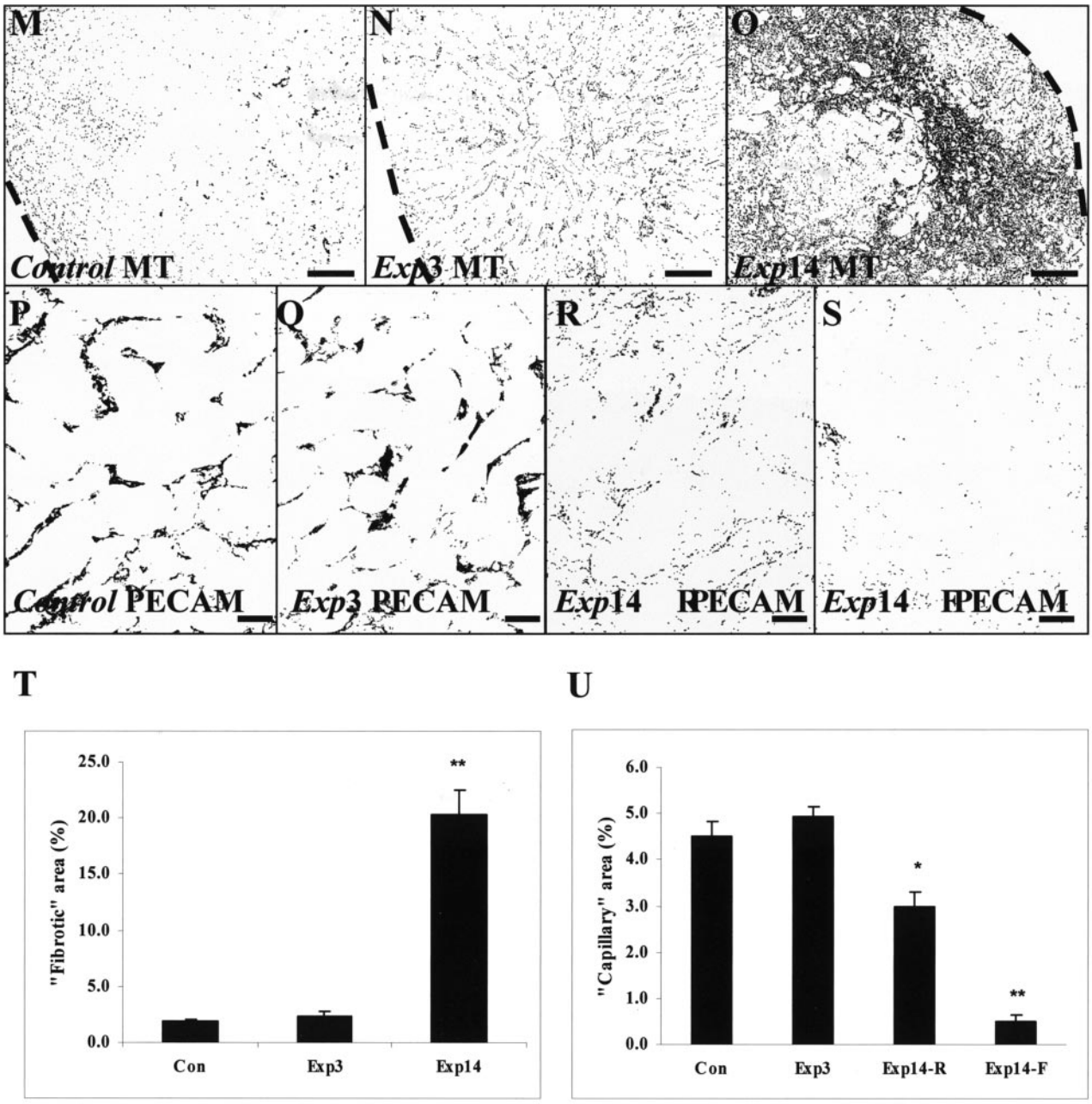

Figure 1. (*Continued*)

detected by chemiluminescence (Amersham Pharmacia Biotech). Negative controls comprised omission of primary antibodies. Proteins were sized with Rainbow markers (Amersham Pharmacia Biotech). The intensities of the resulting bands were measured by densitometry and standardized for protein loading by factoring the major band visualized after exposure to Ponceau S. Note that, in preliminary experiments (data not shown), we found that levels of immunoreactive β-actin, a classic housekeeping protein, were greatly up-regulated during FA nephrotoxicity and therefore could not be used to standardize loading and protein transfer.

Statistic Analyses

Levels of individual proteins or mRNA were compared between groups ($n = 4$ for each Western blots and $n = 3$ for slot blots) using the Mann-Whitney *U*-test, with differences considered significant when P was <0.05.

Results

For all histology results, we report appearances that were representative of all (generally eight) kidneys in any par-

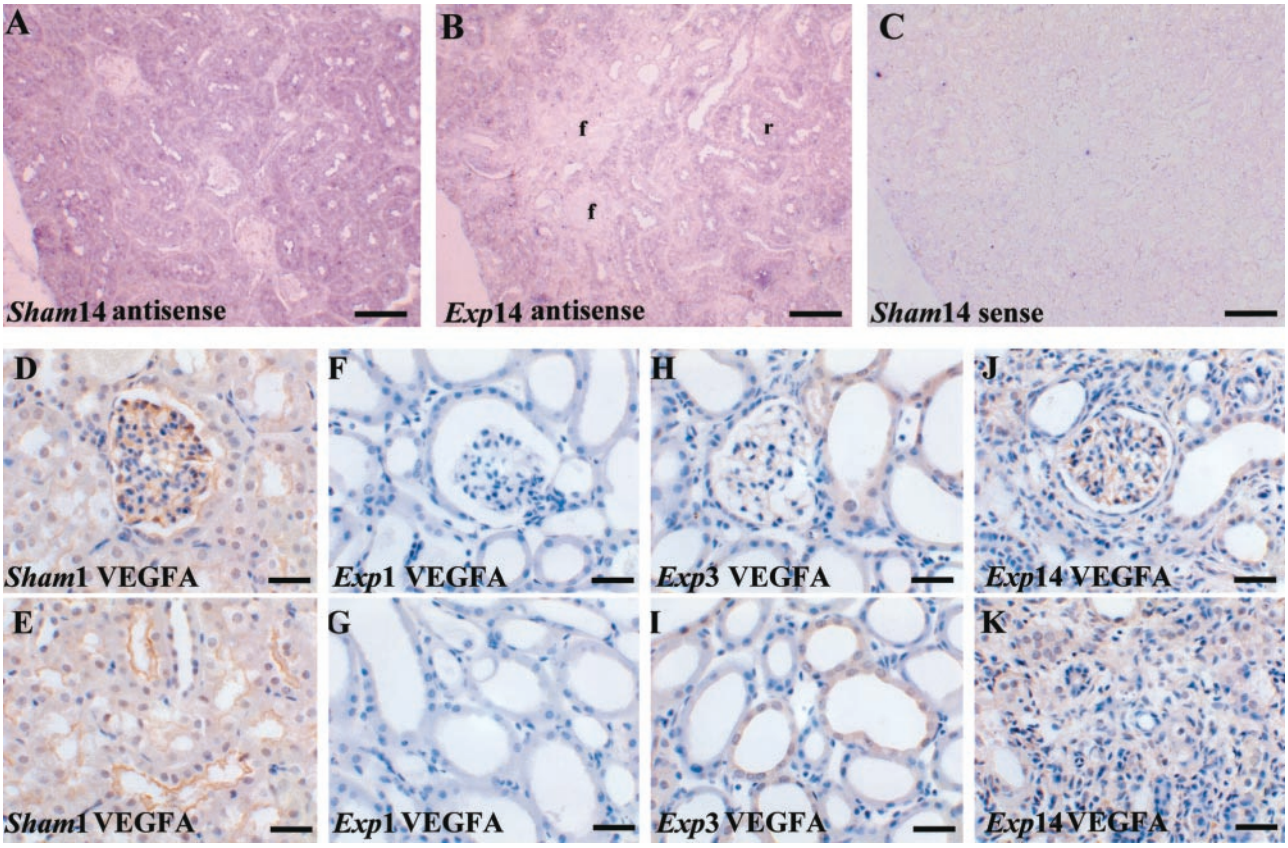

Figure 2. VEGF-A expression in tissue sections. Typical views are shown from eight kidneys in each group. **A** to **C** are VEGF-A *in situ* hybridizations, with **A** and **B** using an anti-sense probe and **C** using a sense probe; a positive signal is indicated by a purple/blue color; **D** to **K** were stained with hematoxylin; **D** to **K** were immunostained (brown) for VEGF-A. **A:** In a day 14 sham sample VEGF-A transcripts were detected mainly in tubule epithelia. **B:** In a day 14 experimental sample VEGF-A transcripts appeared decreased especially in fibrotic areas (f). **C:** Sense control in a sham kidney shows minimal background color. **D** and **E:** VEGF-A immunostaining cells in the periphery of the glomerular tuft (**D**) and in some cortical tubules (**E**) of a sham kidney. **F** and **G:** On experimental day 1 VEGF-A immunostaining was not detected in glomeruli (**F**) and cortical tubules (**G**). **H** and **I:** On experimental day 3 faint VEGF-A immunostaining was detected in some glomeruli (**F**) and dilated cortical tubules (**G**). **J** and **K:** In fibrotic areas, on experimental day 14, faint VEGF-A immunostaining could be detected in glomeruli (**J**) but was absent in atrophied tubules and surrounding fibrotic areas (**K**). Scale bars: 160 μm (**A–C**); 40 μm (**D–K**).

ticular group; furthermore, for any single organ, several sections were examined. No differences were observed between controls and the sham groups. Macroscopically, experimental kidneys appeared pale and swollen on day 1, but then shrank, with cortical depressions apparent by day 14 (data not shown). As described,[5] FA induced severe histological damage visible at days 1 and 3 (Figure 1, A and B) as a uniform flattening of cortical tubule epithelia (ie, acute tubular necrosis). Glomerular tufts were spared, although Bowman's spaces were dilated; in this model of injury, there was also some less prominent, disorganization of medullary structures such as vasa rectae (data not shown).[5] At days 7 and 14, some cortical areas had regenerated with grossly normal tubules (Figure 1C); these regions were separated by areas with atrophic tubules surrounded by interstitium that stained blue with Masson's trichrome, suggesting collagen deposition (Figure 1C). The impression of progressive, patchy cortical interstitial fibrosis was further supported by α-SMA immunostaining; in a typical high-power field, occasional single interstitial cells immunostained (Figure 1D); by experimental day 3, immunoreactive cells were frequently noted between tubules (Figure 1E) and by experimental day 14, the interstitium around atrophic tubules stained intensely for α-SMA (Figure 1F). PECAM immunoreactive capillaries were noted around cortical tubules in all sham groups (Figure 1G) and at experimental days 1 and 3 (Figure 1H and data not shown); by day 14, however, there was qualitatively less immunostaining in fibrotic areas between atrophic tubules (Figure 1I). A similar attrition of capillaries was evident using VEGFR-2 as endothelial marker (Figure 1; J to L). α-SMA immunostaining was not prominent around regenerated tubules and, in these locations, PECAM and VEGFR-2 immunostaining was detected on experimental days 7 and 14 (data not shown). With regard to glomeruli, α-SMA was not up-regulated, nor were PECAM and VEGFR2 down-regulated in the experimental groups (data not shown), consistent with the notion that glomeruli do not undergo major injury in this model. Quantitative image analyses of cortical fibrosis and capillaries using PECAM and Masson's trichrome staining is depicted in Figure 1; M to U. The fibrosis area in control and experimental day 3 groups was minimal (mean of ~2% of total area); on experimental day 14, ~20% of the cortical area was positive. Capillary area was ~4% in the control and experimental day 3 groups; it was modestly decreased (mean ~3%) in regenerated areas at experimental day

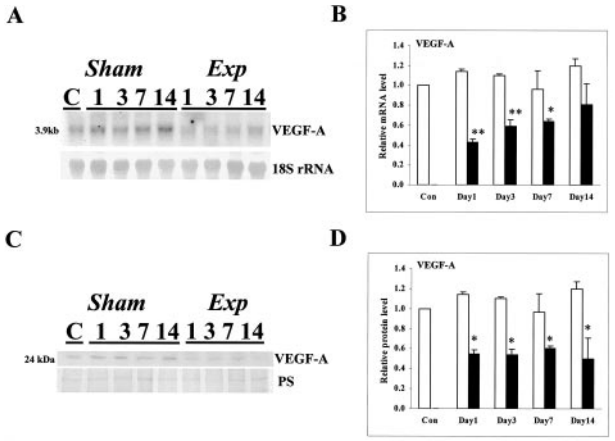

Figure 3. VEGF-A mRNA and protein in whole kidneys. **A:** A representative Northern blot for VEGF-A mRNA and 18S rRNA for sham and experimental samples at days 1, 3, 7, and 14; a control (ie, time = 0 sample) is also depicted. Note the apparently lower signal for VEGF-A (3.9 kb) in all experimental days. **B:** Densitometry for VEGF-A slot blots (factored for 18S rRNA) ($n = 3$). Note that levels were significantly (*, $P < 0.05$; **, $P < 0.01$) reduced in experimental (**solid bars**) *versus* time-matched sham kidneys at days 1, 3, and 7. **C**, **Top**: (*VEGF-A*) shows a representative Western blot (of four experiments) for VEGF-A in sham and experimental samples at days 1, 3, 7, and 14; a control (C) sample is also depicted. A major band was detected at 24 kd. **C**, **Bottom**: Ponceau S staining (*PS*) of the membranes to demonstrate protein loading and transfer. Note the apparently lower signal for VEGF-A in experimental days 1 through 14. **D:** Densitometry for VEGF-A Western blots (factored for PS stain) ($n = 4$) showed that levels were significantly (*, $P < 0.05$) reduced in experimental (**solid bars**) *versus* time-matched sham (**open bars**) kidneys at days 1 through 14.

14 and considerably decreased (<1%) in fibrotic areas at the same time point.

As assessed by *in situ* hybridization, VEGF-A transcripts were detected in the cortex of control and sham kidneys (Figure 2A and data not shown), with the most intense signals over tubules and less intense signals over the periphery of glomerular tufts. At all experimental time points, the intensity of cortical *in situ* hybridization signals were subjectively decreased *versus* time-matched sham kidneys and, on day 14 after FA administration, signals were lower over fibrotic areas *versus* regenerated tubules (Figure 2B and data not shown). Sense probes gave no signal (Figure 2C). VEGF-A immunohistochemistry in control and sham specimens demonstrated protein in glomeruli, mostly in podocytes (Figure 2D), and in some cortical tubules where there was a diffuse cytoplasmic or an apical staining pattern (Figure 2E). At day 1 after FA, no immunostaining could be detected, either in glomeruli (Figure 2F) or in tubules (Figure 2G); from experimental days 3 through 14, VEGF-A immunostaining reappeared in glomeruli and regenerating areas, but remained low or absent in foci of tubulointerstitial disease (Figure 2; H to K). Using Northern blots, we detected a band at 3.9 kb that was less intense in the experimental groups (Figure 3A), and, using slot blots (Figure 3B), VEGF-A mRNA levels factored for 18S rRNA were significantly decreased in experimental *versus* time-matched sham groups on days 1, 3, and 7; at day 14, mean levels were lower in experimental *versus* sham groups but the difference was not significant. Using Western blot, a major VEGF-A band was detected at 24 kd and there was significantly reduced levels in the experimental *versus* sham groups on days 1 through 14 (Figure 3, C and D).

In control and all sham groups, a similar pattern of HIF-1α immunostaining was found with a signal in a subset of glomerular cells, mostly located on the periphery of tufts, consistent with identities as podocytes (Figure 4A), and also in a subset of nuclei in cortical tubules with morphology of proximal and distal tubules (Figure 4, A and B); the latter tubules lacked brush borders, using periodic acid-Schiff staining (data not shown). After FA administration, from day 3 onwards, HIF-1α immunostaining was apparently generally decreased in tubules, especially in areas of atrophy and fibrosis (Figure 4, C and D). With regard to HIF-2α immunostaining, no strong nuclear signal could be detected in control or sham kidneys (Figure 4E and data not shown); instead, a faint cytoplasmic staining was noted. A negative control, with omission of the first antibody, is shown in Figure 4F. In experimental organs, from day 3 onwards, HIF-2α immunostaining was up-regulated in parietal glomerular epithelia, regenerated tubules, where signal was often cytoplasmic as well as nuclear (Figure 4G), and also in atrophic tubules, where the signal was mainly nuclear (Figure 4H). In HIF-1α Western blots of control and sham samples, two major bands were observed at 104 and 94 kd, probably corresponding to isoforms generated by alternative splicing. Both bands appeared less intense in experimental kidneys (Figure 5A), an impression confirmed by densitometry that demonstrated significantly reduced levels in experimental *versus* time-matched sham groups on days 1 through 14 (Figure 5B). In Western blots of all groups (Figure 5A), HIF-2α immunoreactive protein was detected at 118 kd, and the intensity of the band appeared increased at days 3, 7, and 14 after FA administration; densitometry demonstrated significant up-regulation of HIF-2α levels at these time points in experimental *versus* time-matched sham groups (Figure 5C). To explore the hypothesis that HIFs might change at an earlier time point, we also performed Western blot at 12 hours after administration of nephrotoxin and found no significant difference in either HIF-1α or HIF-2α between sham and experimental groups ($n = 3$, data not shown).

In control and sham groups (Figure 6A and data not shown), using an antibody to pimonidazole adducts, a faint immunohistochemical signal was detected in proximal-shaped tubules deep in the cortex and outer medulla; the deep medulla and superficial cortex were immunonegative. The signal intensity was subjectively increased on experimental days 1 through 14. At days 1 and 3, immunostaining was detected in the majority of cortical epithelia that had undergone tubular necrosis (data not shown). At day 14, the experimental kidney cortex remained more hypoxic *versus* the sham (Figure 6, compare B with A); high-power views revealed that hypoxia, as assessed by this assay, was mainly present in proximal-like tubules in regenerated areas (Figure 6C) but, in contrast, hypoxia was not prominent in fibrotic areas (Figure 6D).

In control and sham groups, an immunoreactive band for pVHL was noted at 19 kd, with a fainter band detected at 28 kd in some samples (Figure 7A); these correspond

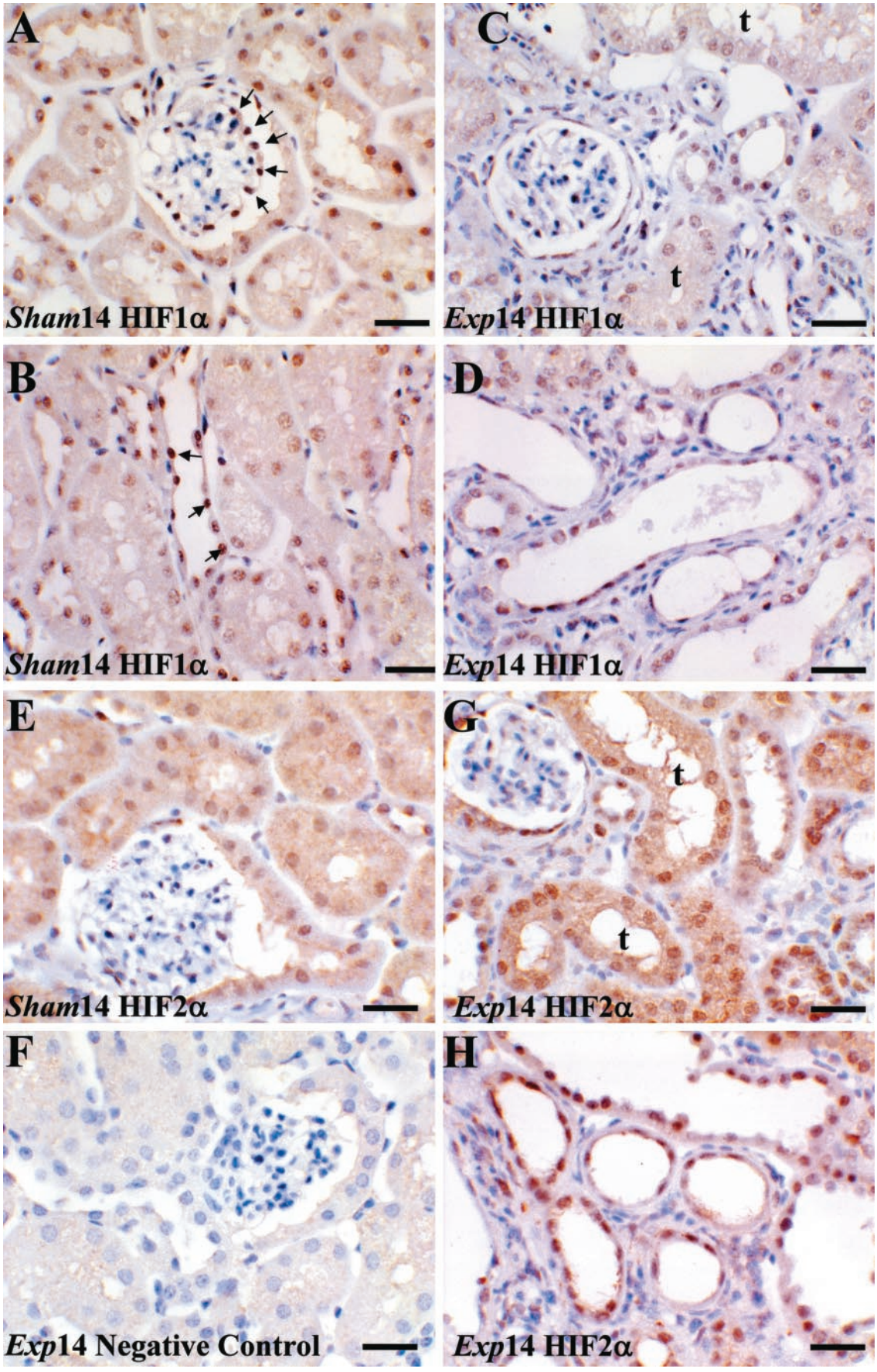
A
*Sham*14 HIF1α
C
t
t
*Exp*14 HIF1α
B
*Sham*14 HIF1α
D
*Exp*14 HIF1α
E
*Sham*14 HIF2α
G
t
t
*Exp*14 HIF2α
F
*Exp*14 Negative Control
H
*Exp*14 HIF2α

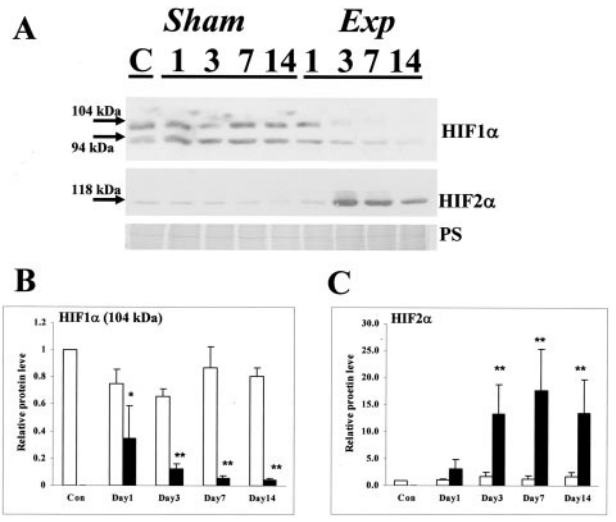

Figure 5. HIF-1α and HIF-2α Western blots of whole kidneys. **A:** Representative Western blot (of four experiments) is depicted. **Top**: A blot for HIF-1α; **middle**: a blot for HIF-2α; **bottom**: Ponceau S staining. With regard to HIF-1α, two major bands (94 and 104 kd) were detected; the intensity of these bands were apparently reduced in the experimental groups, especially on days 3, 7, and 14. With regard to HIF-2α, a band was detected at 118 kd, and this was markedly increased on experimental days 3, 7, and 14. **B:** Densitometry for HIF-1α protein (the 104-kd band factored for PS stain) (n = 4) showed that levels were significantly (*, $P < 0.05$; **, $P < 0.01$) reduced in experimental (**solid bars**) *versus* time-matched sham (**open bars**) kidneys at days 1 through 14. **C:** Densitometry for HIF-2α Western blots (factored for PS stain) (n = 4) showed that levels were significantly (**, $P < 0.01$) increased in experimental (**solid bars**) *versus* time-matched sham (**open bars**) kidneys at days 3, 7, and 14.

to two active forms reported by others.[32] After FA administration the intensity of both bands appeared increased (Figure 7A), an impression confirmed by densitometry, with significant increases in the 28-kd band at days 3, 7, and 14 in the experimental *versus* time-matched sham groups (Figure 7B) and significant increases in the 19-kd band at all experimental times (Figure 7C). In all groups, we detected a 32-kd immunoreactive band for HO-1 and a 30-kd band for EPO (Figure 8A). Using densitometry, there were transient, significant increases in HO-1 (at day 1 in the experimental *versus* time-matched sham groups, Figure 8B) and EPO (at days 1 and 3 in the experimental *versus* time-matched sham groups, Figure 8C).

Discussion

In a previous study, using an identical protocol, we reported that cortical peritubular capillaries undergo limited proliferation, detected by locating proliferating cell nuclear antigen expression in PECAM-immunoreactive cells, in the first few days after FA administration;[5] however, at 7 and 14 days, proliferating peritubular capillaries were not detected. In the current study we demonstrated that, after 14 days, FA nephrotoxicity was associated with attenuation of peritubular capillaries, as assessed by PECAM and VEGFR-2 immunostaining, in areas of cortical tubular atrophy and interstitial fibrosis. We speculate that the apparent attrition of capillaries might be mediated by apoptosis, as demonstrated for glomerular endothelia in other models;[7,33] however, we were unable to prove this mechanism because of technical difficulties in defining apoptotic nuclei in peritubular capillaries by *in situ* end-labeling in PECAM- or VEGFR-2-expressing cells (our unpublished observations). Chronic endothelial loss after acute kidney injury has also been demonstrated in an ischemia model[11,12] but not, to our knowledge, in FA nephrotoxicity. It is possible that, had we continued the period of observation longer, more severe histological progression (eg, glomerulosclerosis) would have ensued; however, the acquisition of patchy tubulointerstitial changes (eg, early fibrosis as assessed by α-SMA expression) by day 14 was striking.

We next assessed the expression of VEGF-A, a molecule with a key role in endothelial survival and growth. In control and sham groups, we found widespread cortical expression of transcripts and protein using *in situ* hybridization and immunohistochemistry. Intensity of these signals fell globally in the cortex on experimental day 1 and remained reduced in areas of tubulointerstitial disease. Because interpretation of *in situ* hybridization and immunostaining intensity is only semiquantitative, we measured VEGF-A in lysates of whole kidneys using slot and Western blots; these analyses confirmed that VEFG-A levels were down-regulated after FA administration, for 7 days in the case of mRNA and for 14 days in the case of protein. One trivial explanation for a lack of VEGF expression could be that kidney tubular cells are severely damaged in the first days after FA and that they experience a biochemical shut-down and global decrease in gene expression. This contention cannot be supported, however, because we previously demonstrated that most regeneration, as assessed by thymidine incorporation, occurs in the first 48 hours after FA administration[26] and other genes such as angiopoietin-1 and Pax-2 are actually up-regulated in tubule epithelia in this time frame.[5,34] Similarly, although release of VEGF-A from damaged epithelia and extracellular sequestration could be an explanation for decreased tubular immunostaining, this would not explain the fall of VEGF-A protein in lysates of snap-frozen kidneys.

Kang and colleagues[9,10] demonstrated a decrease in VEGF expression after subtotal nephrectomy in adult rats that correlated with overall loss of capillaries and they further showed that administration of the factor attenu-

Figure 4. HIF immunohistochemistry. Typical views are shown from eight kidneys in each group. **A** to **H** were stained with hematoxylin; **A** to **D** were immunostained (brown) for HIF-1α; **E**, **G**, and **H** were immunostained for HIF-2α; in **F**, the primary antibody was omitted. **A** and **B:** In day 14 sham sections, HIF-1α immunoreactivity was noted in glomeruli, especially in presumed podocytes on the periphery of glomerular tufts (**arrows** in **A**). Positive signal was also found in some nuclei of cortical tubules, including those with typical morphology of proximal and also distal tubules (**arrows** in **B**). **C** and **D:** In fibrotic locations in day 14 experimental sections, HIF-1α immunoreactivity appeared decreased in glomeruli (**C**) and in epithelia of regenerated (t in **C**) atrophic tubules (**D**). **E:** In day 14 sham sections, HIF-2α immunoreactivity was weak in tubules or absent in glomeruli. **F:** Shows a section of a experimental day 14 kidney, in which the primary antibody was omitted. **G** and **H:** On experimental day 14, HIF-2α immunostaining was prominent in some regenerated proximal tubules (t in **G**) and in parietal glomerular epithelia (**G**), and additionally in nuclei of epithelia of atrophic tubules in fibrotic areas (**H**). Scale bars, 40 μm.

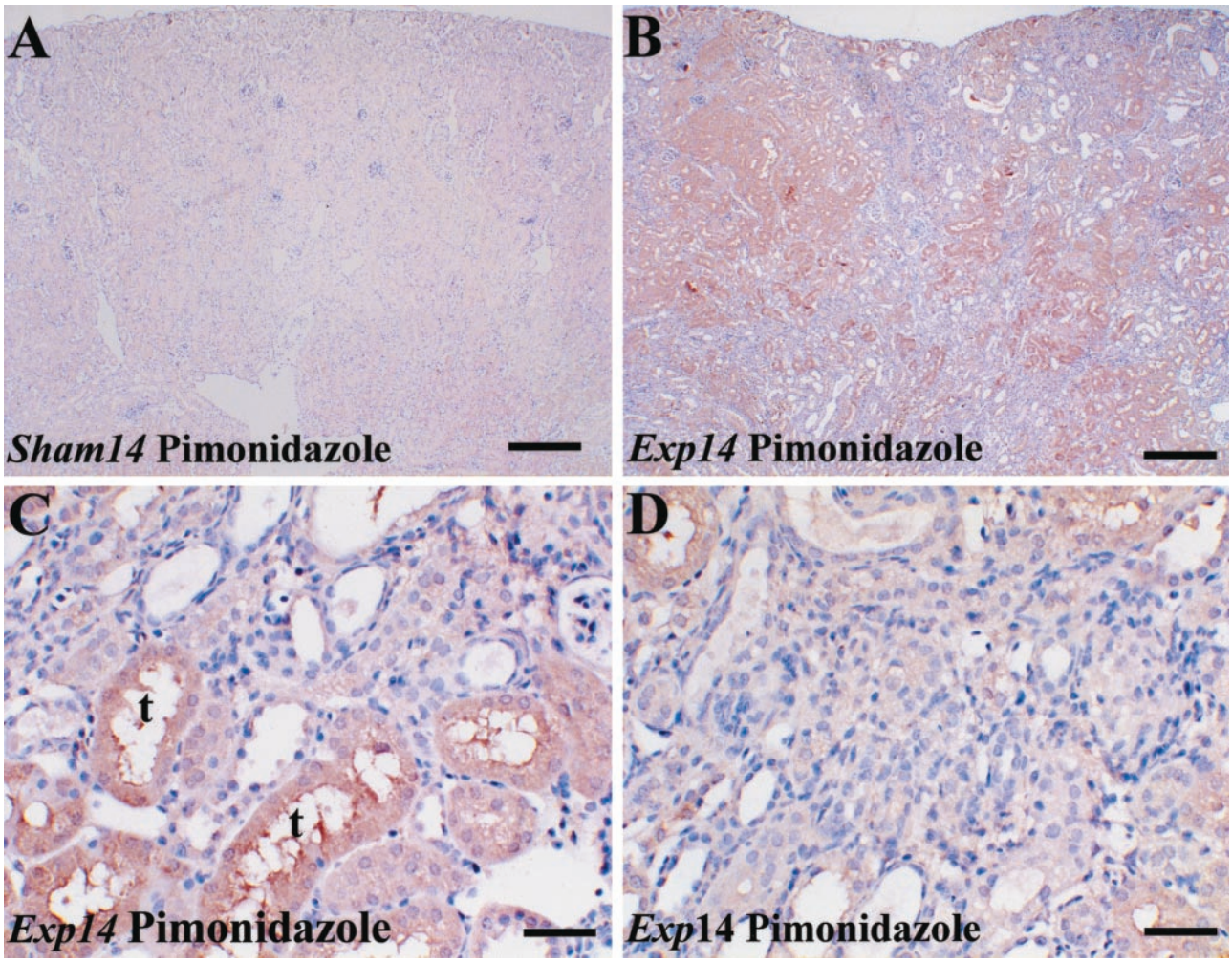

Figure 6. *In situ* detection of hypoxia. Typical views are shown from four kidneys in each group at day 14. **A** to **D** were stained with hematoxylin and immunoprobed for pimonidazole adducts in animals injected with Hypoxyprobe-1. **A:** In a sham kidney (**A**), faint immunohistochemical signal (brown) was detected in proximal tubules deep in the cortex. The intensity of the signal was subjectively increased in parts of the cortex after FA administration (**B**). **C** and **D** are high-power views of the experimental kidney cortex, showing prominent signal in regenerated tubules with a proximal morphology (**C**), but little signal in a fibrotic location (**D**). Omitting primary antibody resulted in no signal (not shown). Scale bars: 320 μm (**A** and **B**); 40 μm (**C** and **D**).

ated renal damage. On the other hand, Pillebout and colleagues,[8] using subtotal nephrectomy in mice, found that VEGF protein levels actually increased and that this was correlated with peritubular capillary growth; furthermore, the magnitude of these effects was strain-dependent. Clearly, then there are no stereotypic responses with regard to either peritubular capillary remodeling or VEGF expression after renal injury, and instead the precise responses must be determined by the type and severity of the insult, as well as by (poorly understood) species and strain influences. In addition, one can postulate that the age of an experimental animal might modify responses based on the data presented by Rivard and colleagues[35] in which VEGF expression was studied in aortic rings harvested from young and older rabbits.

HIF proteins are regulators of VEGF expression[36] and HIF-α levels and activities are generally determined by alterations of protein stability.[21–23] Therefore, we assessed expression of HIF-1α and HIF-2α in the FA model. Using immunohistochemistry, HIF-1α was expressed at low levels in control and sham kidneys, whereas HIF-2α was hardly detectable. Furthermore, we observed an apparent decrease in HIF-1α immunostaining and an apparent increase in HIF-2α immunostaining in the experimental groups. Most immunostaining for both proteins was in nuclei or cytoplasm of epithelia. HIF-1α and HIF-2α proteins levels can change rapidly; for example, they can be up-regulated within minutes in cultured cells and they can be degraded throughout several minutes when oxygen tensions increase.[37] We considered that it was theoretically possible that our immunohistochemical results could have been influenced by the period between harvest and complete *ex vivo* organ fixation. Therefore, we quantified HIF-α proteins in Western blots of kidneys snap-frozen in liquid nitrogen harvested within 1 minute of death. Taking the immunohistochemical and Western blot data together, FA nephrotoxicity was associated with an overall down-regulation of HIF-1α immunoreactive protein and up-regulation of HIF-2α immunoreactive protein.

There is some debate regarding the occurrence, and specific location of, HIF-α protein in normal murine kid-

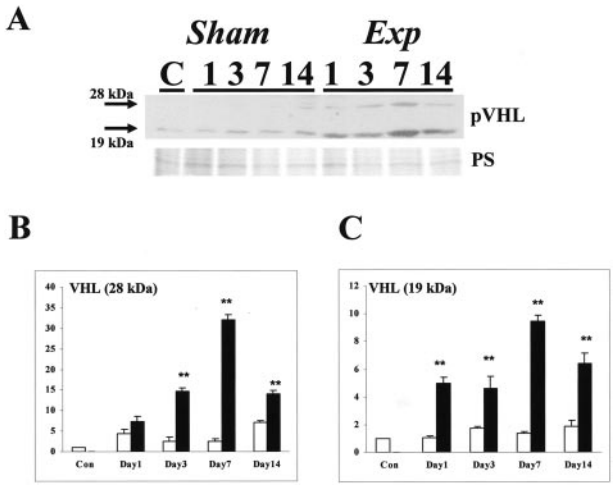

Figure 7. Western blot for pVHL. **A:** A representative Western blot (of four experiments) is depicted. **Top**: Blot for pVHL; **bottom**: Ponceau S staining. With regard to pVHL, two immunoreactive major bands (19 and 28 kd) were detected; the intensities of these bands were apparently increased in the experimental groups. **B:** Densitometry for pVHL (the 28-kd band factored for PS stain) ($n = 4$) showed that levels were significantly (**, $P < 0.01$) increased in experimental (**solid bars**) *versus* time-matched sham (**open bars**) kidneys at days 3, 7, and 14. **C:** Densitometry for pVHL (the 19-kd band factored for PS stain) ($n = 4$) showed that levels were significantly (**, $P < 0.01$) increased in experimental *versus* time-matched sham kidneys at days 1 through 14.

neys. Ema and colleagues[38] detected HIF-1α and HIF-2α mRNA in adult mice kidneys using Northern blots. Stroka and colleagues[37] reported that, in adult mice, HIF-1α immunolocalized to distal convoluted tubules, and that cytoplasmic and nuclear signals were increased in systemic hypoxia; using Western blots, HIF-1α increased transiently with hypoxia. Freeburg and colleagues[39] studied immature mouse kidneys and found, by *in situ* hybridization, that HIF-1α and HIF-2α were expressed in the

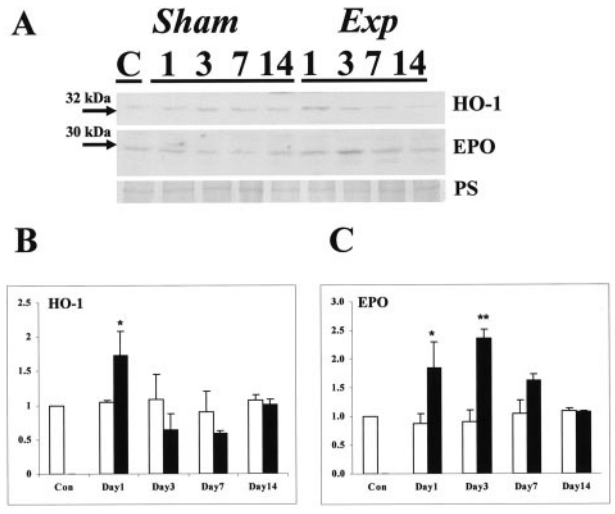

Figure 8. Western blot for HO-1 and EPO. **A:** A representative Western blot (of four experiments) is depicted. **Top**: blot for HO-1 (32 kd); **middle**: blot for EPO (30 kd); **bottom**: Ponceau red staining. **B:** Densitometry for HO-1 protein (the factored for PS stain) ($n = 4$) showed that levels were significantly (*, $P < 0.05$) increased in experimental *versus* time-matched sham kidneys at day 1. **C:** Densitometry for EPO protein (factored for PS stain) ($n = 4$) showed that levels were significantly (*, $P < 0.05$ and **, $P < 0.01$) increased in experimental *versus* time-matched sham kidneys at days 1 and 3.

Table 1. Overview of Changes in VEGF-A and HIF Immunohistochemistry and *in Situ* Hypoxia

	Early (day 3 after FA)	Late (day 14 after FA)
VEGFA	General decrease	Recovery in regenerated tubules, low in fibrotic areas
HIF-1α	General decrease	General decrease
HIF-2α	General increase	General increase
In situ hypoxia	General increase	Increase in regenerated tubules

Changes refer to histological observations in the renal cortex of experimental *versus* time-matched sham groups.

nephrogenic zone and medulla of neonates, and HIF-2α immunolocalized to maturing podocytes and tubules. Abdulmalek and colleagues[40] detected abundant HIF-1α mRNA in kidneys of normoxic rats, and this was increased by hypoxia. Rosenberger and colleagues[41] used immunohistochemistry of perfusion-fixed kidneys of adult rats and failed to detect HIF-α proteins in normoxia; using various models of systemic hypoxia, HIF-1α protein was induced in tubular cells (typically in connecting tubules and collecting ducts) and co-localized with HO-1; with systemic hypoxia, HIF-2α was immunolocalized to nontubular cells (eg, endothelia of glomeruli, peritubular endothelia, and fibroblasts). Others,[42] on the other hand, did detect low levels of HIF-1α in normal rat kidneys. Most likely, some of the variation in results is explained by examination of different species (or even strains of animals) using different methodologies of different sensitivities; we consider that the data from mouse kidney studies are more relevant to our model.

If we accept that HIF-1α protein falls after FA administration, then this correlates with VEGF-A down-regulation. On the other hand, from experimental day 3, tubule HIF-2α expression was increased; this introduces a paradox because both HIF-α proteins can stimulate VEGF transcription.[21–23] One explanation to reconcile these observations is that VEGF levels are modulated by several inputs, not just by HIF-α proteins; indeed, stress-activated protein kinases stabilize VEGF transcripts, several growth factors, and oncogenic transformation activates the VEGF promoter, whereas wild-type p53 suppresses VEGF transcription.[20,43] In the future, it would be interesting to examine some of these variables in the FA model. In fact, in other organs, HIF expression does not invariably correlate with VEGF expression, suggesting other roles for these factors.[44] Although it is thought that HIF-1α and HIF-2α have mostly common transcriptional targets, there is evidence that HIF-2α activates the angiopoietin receptor Tie-2[45] and intriguingly Tie-2 protein levels tend to increase in the 2 weeks after FA-induced kidney damage.[5] In the current study, we also found that EPO and HO-1, two established hypoxia/HIF-α targets, did indeed increase transiently, as assessed by Western blots, in the first days after FA administration. It is interesting to note that, as assessed by Western blot,

changes in HIF-1α, HIF-2α, HO-1, and EPO expression were asynchronous, demonstrating that each of these hypoxia-responsive proteins must be under complex, perhaps regional, individual controls.

Oxygen regulates the stability of HIF-α proteins, with low tensions stabilizing these proteins by preventing their degradation. We therefore used the Hypoxyprobe-1 kit to establish whether renal tissues were hypoxic. Table 1 gives an overview of changes in VEGF-A and HIF immunohistochemistry and *in situ* hypoxia in the renal cortex in experimental *versus* time-matched sham groups. We found that there was an increase of hypoxia after FA, and this was especially evident in regenerating tubules, whereas areas of atrophy and fibrosis were not immunoreactive for pimonidazole adducts. If we accept that such signals represent foci of real hypoxia, it may explain the up-regulation of HIF-2α, at least in regenerated proximal tubules. HIF-2α was also seen to be up-regulated in fibrotic/atrophic areas that did not appear hypoxic by Hypoxyprobe-1. With regard to the latter observation, we speculate that availability of the biomarker, which must depend on blood perfusion, may be limited in areas of fibrosis and capillary fall-out; hence, we remain cautious about ruling out hypoxia in such locations using this assay. In addition, we can only speculate why the same degree of hypoxia in regenerated proximal tubules was manifestly not associated with up-regulation of HIF-1α protein. Is it possible that HIF-α levels are regulated by factors unrelated to hypoxia; moreover, do some conditions affect HIF-1α and HIF-2α levels differently? As affirmative answers to these questions, Agani and colleagues[46] found that nitric oxide donors prevented HIF-1α accumulation in hypoxic cultured cells, and Isaacs and colleagues[47] noted that disruption of heat shock protein 90 function promoted HIF-1α degradation via an oxygen-independent E3 ubiquitin ligase. Furthermore, in mouse uteri, progesterone primarily up-regulated HIF-1α mRNA, whereas estrogen increased HIF-2α mRNA,[44] and LY294002, a phosphatidylinositol 3′-kinase inhibitor, inhibited hypoxia-induction of HIF-1α in breast cancer cells, whereas the up-regulation of HIF-2α was unaffected.[48] It is also important to note that tissue hypoxia may directly contribute to progressive renal damage; for example, Orphanides and colleagues[49] reported that, *in vitro*, hypoxia stimulates the production of matrix components by proximal tubule cells.

pVHL has a role in destabilizing HIF-1α and HIF-2α; we therefore measured pVHL using Western blot and found that the 29-kd and 19-kd isoform increased significantly in the experimental groups; this may provide one explanation for the fall of HIF-1α. Mandriota and colleagues[50] found that, in patients with germline defunctioning mutations of *VHL*, HIF activation was an early event occurring in morphologically normal single cells in renal tubules; in normal kidneys, pVHL was expressed by distal and proximal tubules, and somatic loss of the remaining VHL allele was associated with up-regulation of VEGF; HIF-1α was up-regulated in morphologically normal foci of pVHL loss, whereas HIF-2α was increased in cysts and regions of overt cancer. Preliminary studies (data not shown) in our model, using the tissue preparation described in Materials and Methods, failed to generate immunostaining, so localization of these proteins to specific cells within the normal and injured mouse kidney was not possible.

Conclusions

Hence, levels of HIF-2α, HO-1, EPO, and pVHL respond differently after nephrotoxic injury when compared to VEGF-A and HIF-1α, with the former group significantly increasing, and the latter group significantly decreasing after FA administration. We speculate that that down-regulation of VEGF-A may be functionally-implicated in the progressive attrition of peritubular capillaries in areas of tubular atrophy and interstitial fibrosis; VEGF-A down-regulation correlates with a loss of HIF-1α expression which itself occurs in the face of increased tissue hypoxia.

References

1. Hammerman MR: Growth factors and apoptosis in acute renal injury. Curr Opin Nephrol Hypertens 1998, 7:419–424
2. Sheridan AM, Bonventre JV: Cell biology and molecular mechanisms of injury in ischemic acute renal failure. Curr Opin Nephrol Hypertens 2000, 9:427–434
3. Romanov V, Noiri E, Czerwinski G, Finsinger D, Kessler H, Goligorsky MS: Two novel probes reveal tubular and vascular Arg-Gly-Asp (RGD) binding sites in the ischemic rat kidney. Kidney Int 1997, 52:93–102
4. Brodsky SV, Yamamoto T, Tada T, Kim B, Chen J, Kajiya F, Goligorsky MS: Endothelial dysfunction in ischemic acute renal failure: rescue by transplanted endothelial cells. Am J Physiol 2002, 282:F1140–F1149
5. Long DA, Woolf AS, Suda T, Yuan HT: Increased renal angiopoietin-1 expression in folic acid-induced nephrotoxicity in mice. J Am Soc Nephrol 2001, 12:2721–2731
6. Kang DH, Kanellis J, Hugo C, Truong L, Anderson S, Kerjaschki D, Schreiner GF, Johnson RJ: Role of the microvascular endothelium in progressive renal disease. J Am Soc Nephrol 2002, 13:806–816
7. Kitamura H, Shimizu A, Masuda Y, Ishizaki M, Sugisaki Y, Yamanaka N: Apoptosis in glomerular endothelial cells during the development of glomerulosclerosis in the remnant-kidney model. Exp Nephrol 1998, 6:328–336
8. Pillebout E, Burtin M, Yuan HT, Briand P, Woolf AS, Friedlander G, Terzi F: Proliferation and remodeling of the peritubular microcirculation after nephron reduction: association with the progression of renal lesions. Am J Pathol 2001, 159:547–560
9. Kang DH, Hughes J, Mazzali M, Schreiner GF, Johnson RJ: Impaired angiogenesis in the remnant kidney model: II. Vascular endothelial growth factor administration reduces renal fibrosis and stabilizes renal function. J Am Soc Nephrol 2001, 12:1448–1457
10. Kang DH, Joly AH, Oh SW, Hugo C, Kerjaschki D, Gordon KL, Mazzali M, Jefferson JA, Hughes J, Madsen KM, Schreiner GF, Johnson RJ: Impaired angiogenesis in the remnant kidney model: I. Potential role of vascular endothelial growth factor and thrombospondin-1. J Am Soc Nephrol 2001, 12:1434–1447
11. Basile DP, Donohoe D, Roethe K, Osborn JL: Renal ischemic injury results in permanent damage to peritubular capillaries and influences long-term function. Am J Physiol 2001, 281:F887–F899
12. Basile DP, Donohoe DL, Roethe K, Mattson DL: Chronic renal hypoxia after acute ischemic injury: effects of L-arginine on hypoxia and secondary damage. Am J Physiol 2003, 284:F338–F348
13. Seron D, Alexopoulos E, Raftery MJ, Hartley B, Cameron JS: Number of interstitial capillary cross-sections assessed by monoclonal antibodies: relation to interstitial damage. Nephrol Dial Transplant 1990, 5:889–893
14. Bohle A, Mackensen-Haen S, Wehrmann M: Significance of postglomerular capillaries in the pathogenesis of chronic renal failure. Kidney Blood Press Res 1996, 19:191–195
15. Konda R, Sato H, Sakai K, Sato M, Orikasa S, Kimura N: Expression

of platelet-derived endothelial cell growth factor and its potential role in up-regulation of angiogenesis in scarred kidneys secondary to urinary tract diseases. Am J Pathol 1999, 155:1587–1597
16. Conway EM, Collen D, Carmeliet P: Molecular mechanisms of blood vessel growth. Cardiovasc Res 2001, 49:507–521
17. Brown LF, Berse B, Tognazzi K, Manseau EJ, Van de WL, Senger DR, Dvorak HF, Rosen S: Vascular permeability factor mRNA and protein expression in human kidney. Kidney Int 1992, 42:1457–1461
18. Loughna S, Hardman P, Landels E, Jussila L, Alitalo K, Woolf AS: A molecular and genetic analysis of renal glomerular capillary development. Angiogenesis 1997, 1:84–101
19. Woolf AS, Yuan HT: The development of kidney blood vessels. The Kidney: from Normal Development to Congenital Disease. Edited by PD Vize, AS Woolf, JBL Bard. Elsevier Science/Academic Press, 2003, pp 251–266
20. Mazure NM, Brahimi-Horn MC, Pouyssegur J: Protein kinases and the hypoxia-inducible factor-1, two switches in angiogenesis. Curr Pharm Des 2003, 9:531–541
21. Safran M, Kaelin Jr WG: HIF hydroxylation and the mammalian oxygen-sensing pathway. J Clin Invest 2003, 111:779–783
22. Huang LE, Bunn HF: Hypoxia-inducible factor and its biomedical relevance. J Biol Chem 2003, 278:19575–19578
23. Pugh CW, Ratcliffe PJ: The von Hippel-Lindau tumor suppressor, hypoxia-inducible factor-1 (HIF-1) degradation, and cancer pathogenesis. Semin Cancer Biol 2003, 13:83–89
24. Mullin EM, Bonar RA, Paulson DF: Acute tubular necrosis. An experimental model detailing the biochemical events accompanying renal injury and recovery. Invest Urol 1976, 13:289–294
25. Fink M, Henry M, Tange JD: Experimental folic acid nephropathy. Pathology 1987, 19:143–149
26. Bosch RJ, Woolf AS, Fine LG: Gene transfer into the mammalian kidney: direct retrovirus-transduction of regenerating tubular epithelial cells. Exp Nephrol 1993, 1:49–54
27. Lee YM, Jeong CH, Koo SY, Son MJ, Song HS, Bae SK, Raleigh JA, Chung HY, Yoo MA, Kim KW: Determination of hypoxic region by hypoxia marker in developing mouse embryos in vivo: a possible signal for vessel development. Dev Dyn 2001, 220:175–186
28. Yuan HT, Suri C, Yancopoulos GD, Woolf AS: Expression of angiopoietin-1, angiopoietin-2, and the Tie-2 receptor tyrosine kinase during mouse kidney maturation. J Am Soc Nephrol 1999, 10:1722–1736
29. Yuan HT, Gowan S, Kelly FJ, Bingle CD: Cloning of guinea pig surfactant protein A defines a distinct cellular distribution pattern within the lung. Am J Physiol 1997, 273:L900–L906
30. Yuan HT, Bingle CD, Kelly FJ: Differential patterns of antioxidant enzyme mRNA expression in guinea pig lung and liver during development. Biochim Biophys Acta 1996, 1305:163–171
31. Yuan HT, Yang SP, Woolf AS: Hypoxia up-regulates angiopoietin-2, a Tie-2 ligand, in mouse mesangial cells. Kidney Int 2000, 58:1912–1919
32. Iliopoulos O, Ohh M, Kaelin Jr WG: pVHL19 is a biologically active product of the von Hippel-Lindau gene arising from internal translation initiation. Proc Natl Acad Sci USA 1998, 95:11661–11666
33. Yuan HT, Tipping PG, Li XZ, Long DA, Woolf AS: Angiopoietin correlates with glomerular capillary loss in anti-glomerular basement membrane glomerulonephritis. Kidney Int 2002, 61:2078–2089
34. Imgrund M, Grone E, Grone HJ, Kretzler M, Holzman L, Schlondorff D, Rothenpieler UW: Re-expression of the developmental gene Pax-2 during experimental acute tubular necrosis in mice 1. Kidney Int 1999, 56:1423–1431
35. Rivard A, Berthou-Soulie L, Principe N, Kearney M, Curry C, Branellec D, Semenza GL, Isner JM: Age-dependent defect in vascular endothelial growth factor expression is associated with reduced hypoxia-inducible factor 1 activity. J Biol Chem 2000, 275:29643–29647
36. Iyer NV, Kotch LE, Agani F, Leung SW, Laughner E, Wenger RH, Gassmann M, Gearhart JD, Lawler AM, Yu AY, Semenza GL: Cellular and developmental control of O_2 homeostasis by hypoxia-inducible factor 1α. Genes Dev 1998, 12:149–162
37. Stroka DM, Burkhardt T, Desbaillets I, Wenger RH, Neil DA, Bauer C, Gassmann M, Candinas D: HIF-1 is expressed in normoxic tissue and displays an organ-specific regulation under systemic hypoxia. FASEB J 2001, 15:2445–2453
38. Ema M, Taya S, Yokotani N, Sogawa K, Matsuda Y, Fujii-Kuriyama Y: A novel bHLH-PAS factor with close sequence similarity to hypoxia-inducible factor 1alpha regulates the VEGF expression and is potentially involved in lung and vascular development. Proc Natl Acad Sci USA 1997, 94:4273–4278
39. Freeburg PB, Robert B, St John PL, Abrahamson DR: Podocyte expression of hypoxia-inducible factor (HIF)-1 and HIF-2 during glomerular development. J Am Soc Nephrol 2003, 14:927–938
40. Abdulmalek K, Ashur F, Ezer N, Ye F, Magder S, Hussain SN: Differential expression of Tie-2 receptors and angiopoietins in response to in vivo hypoxia in rats. Am J Physiol 2001, 281:L582–L590
41. Rosenberger C, Mandriota S, Jurgensen JS, Wiesener MS, Horstrup JH, Frei U, Ratcliffe PJ, Maxwell PH, Bachmann S, Eckardt KU: Expression of hypoxia-inducible factor-1α and -2α in hypoxic and ischemic rat kidneys. J Am Soc Nephrol 2002, 13:1721–1732
42. Zou AP, Yang ZZ, Li PL, Cowley Jr AW: Oxygen-dependent expression of hypoxia-inducible factor-1α in renal medullary cells of rats. Physiol Genomics 2001, 6:159–168
43. Zhang L, Yu D, Hu M, Xiong S, Lang A, Ellis LM, Pollock RE: Wild-type p53 suppresses angiogenesis in human leiomyosarcoma and synovial sarcoma by transcriptional suppression of vascular endothelial growth factor expression. Cancer Res 2000, 60:3655–3661
44. Daikoku T, Matsumoto H, Gupta RA, Das SK, Gassmann M, DuBois RN, Dey SK: Expression of hypoxia-inducible factors in the periimplantation mouse uterus is regulated in a cell-specific and ovarian steroid hormone-dependent manner. Evidence for differential function of HIFs during early pregnancy. J Biol Chem 2003, 278:7683–7691
45. Tian H, McKnight SL, Russell DW: Endothelial PAS domain protein 1 (EPAS1), a transcription factor selectively expressed in endothelial cells. Genes Dev 1997, 11:72–82
46. Agani FH, Puchowicz M, Chavez JC, Pichiule P, LaManna J: Role of nitric oxide in the regulation of HIF-1α expression during hypoxia. Am J Physiol 2002, 283:C178–C186
47. Isaacs JS, Jung YJ, Mimnaugh EG, Martinez A, Cuttitta F, Neckers LM: Hsp90 regulates a von Hippel Lindau-independent hypoxia-inducible factor-1α degradative pathway. J Biol Chem 2002, 277:29936–29944
48. Blancher C, Moore JW, Robertson N, Harris AL: Effects of ras and von Hippel-Lindau (VHL) gene mutations on hypoxia-inducible factor (HIF)-1alpha, HIF-2alpha, and vascular endothelial growth factor expression and their regulation by the phosphatidylinositol 3′-kinase/Akt signaling pathway. Cancer Res 2001, 61:7349–7355
49. Orphanides C, Fine LG, Norman JT: Hypoxia stimulates proximal tubular cell matrix production via a TGF-β1-independent mechanism. Kidney Int 1997, 52:637–647
50. Mandriota SJ, Turner KJ, Davies DR, Murray PG, Morgan NV, Sowter HM, Wykoff CC, Maher ER, Harris AL, Ratcliffe PJ, Maxwell PH: HIF activation identifies early lesions in VHL kidneys: evidence for site-specific tumor suppressor function in the nephron. Cancer Cell 2002, 1:459–468